International Journal of Pharmaceutics 408 (2011) 67–75

Contents lists available at ScienceDirect

International Journal of Pharmaceutics

journal homepage: www.elsevier.com/locate/ijpharm

A cocktail of metabolic probes demonstrates the relevance of primary human hepatocyte cultures in a microfluidic biochip for pharmaceutical drug screening

Jean-Matthieu Prot[a], Orianne Videau[b], Céline Brochot[c], Cécile Legallais[a], Henri Bénech[b], Eric Leclerc[a,*]

[a] CNRS UMR 6600, Laboratoire de Biomécanique et Bioingénierie, Université de Technologie de Compiègne, France
[b] CEA, iBitecS, Service de Pharmacologie et d'Immunoanalyse, Laboratoire d'Etude du Métabolisme et du Médicament, 91191 Gif-sur-Yvette Cedex, France
[c] Institut National de l'Environnement Industriel et des Risques (INERIS), Unité Modèles pour l'Ecotoxicoclogie et la Toxicologie, Parc ALATA, BP2, 60550 Verneuil en Halatte, France

ARTICLE INFO

Article history:
Received 2 November 2010
Received in revised form 21 January 2011
Accepted 25 January 2011
Available online 1 February 2011

Keywords:
Metabolism
CIME cocktail
Human primary hepatocytes
Microfluidic
Biochip
Drug screening

ABSTRACT

In this paper, we compare the biotransformation capacities of cryopreserved primary human hepatocytes cultivated in a liver microfluidic biochip and in plates. The hepatocytes were exposed to the CIME cocktail (Carte d'Identité MEtabolique), a mixture of seven probes (acetaminophen, amodiaquine, caffeine, dextromethorphan, midazolam, omeprazole and tolbutamide) for key enzymes involved in the xenobiotic metabolism and pharmacokinetics. The purpose of the cocktail was to give an overview of the metabolic profile of the hepatocytes due to concomitant exposure and a simultaneous mass spectrometric detection method of the metabolites. The results showed a greater activity for CYP1A2, CYP2C9, CYP2C19 CYP2D6, CYP3A and UGT1A1 after 4 h of incubation in the microfluidic biochip when compared to the plate cultures. Furthermore, the metabolic ratio time-course measured at 1 h, 3 h and 4 h indicated that the enzymatic activity increased when the hepatocytes were cultivated in the microfluidic biochip, in contrast with their response in the plate cultures. These results illustrated the functional relevance of liver culture in the PDMS microfluidic biochip. The original method based on a microfluidic culture coupled with CIME cocktail analysis allowed the maintenance and the evaluation of the metabolic performances of the primary human hepatocytes through a new rapid assay. This metabolic analysis can thus become the reference situation when parallel studies of drug metabolism and toxicities are planned with functional hepatocytes in biochips.

1. Introduction

Metabolism is one of the most important pharmacokinetic processes affecting the presence and elimination of drugs and xenobiotics in the human body. Drugs and xenobiotics are metabolized by various oxidation and conjugation enzymes to more polar and soluble metabolites in order to facilitate their excretion from the body. However, metabolism is not only involved in detoxification. In some cases, metabolism can also lead to the generation of chemically reactive metabolites which can potentially induce toxic effects or be responsible for pharmacological effects, as is the case with prodrugs. With a possible link between reactive metabolites and adverse or pharmacological effects, screening for the metabolic activation of drug candidates has become an essential step in the drug discovery process (Baillie, 2006; Erve, 2006)

The liver plays a major role in the biotransformation of drugs and xenobiotics through high levels of metabolizing enzymes and also the first pass effect for drugs given *per os*. Hepatocytes are considered to be one of the best models in *in vitro* pharmacological studies (Gomez-Lechon et al., 2007; Guillouzo et al., 1997; LeCluyse, 2001; Maurel, 1996). Hepatocytes effectively have the major drug metabolism enzymes devoted to biotransformation, such as cytochromes P450 (CYPs), glutathione transferases, sulfotransferases, glucuronosyltransferases and several drug transporters. Many different authors have already investigated the effects of drugs on the induction or repression of these enzymes, the kinetics of appearance and depletion of drugs and their reaction products, and the determination of the intrinsic clearance of each molecule (Hewitt and Hewitt, 2004; Kedderis and Held, 1996; Lau et al., 2002; Lipscomb and Poet, 2008; Soars et al., 2007).

Abbreviations: CIME, carte d'Identité MEtabolique; CYP450, cytochrome P450; UGT, uridine diphosphate glucuronosyltransferase; UGT 1A1, uridine diphosphate-glucuronosyltransferase 1 polypeptide 1A; UGT 2B7, uridine diphosphate-glucuronosyltransferase 2 polypeptide 7B; SULT, sulfotransferase; MDR1, multi drug resistance protein 1; MRP2m, ulti drug resistance-associated protein 2; PDMS, polydimethylsiloxane; 1OHMDZ, 1-OH-midazolam; 4OHMDZ, 4-OH-midazolam; PARA, paraxanthine; 4OHTOLB, 4-OH-tolbutamide; ACEGLU, acetaminophen glucuronide; DESE, desethylamodiaquine; MEM, 3-methoxymorphinan; DXR, dextorphan; 5OHOME, 5-OH-omeprazole; OMESU, omeprazole-sulfone.

* Corresponding author. Tel.: +33344237943; fax: +33344237942.
E-mail address: eric.leclerc@utc.fr (E. Leclerc).

0378-5173/$ – see front matter © 2011 Elsevier B.V. All rights reserved.
doi:10.1016/j.ijpharm.2011.01.054

Unfortunately, hepatocytes rapidly lose a wide range of their specific detoxification functions when they are cultivated in 2D static conditions or in suspension (Hewitt et al., 2007). Therefore, new approaches have been proposed to maintain their differentiation status. A collagen gel sandwich, matrigel™ and spheroids have been widely used to make 3D cell organisation possible (Brandon et al., 2003; Richert et al., 2010; Kienhuis et al., 2007). Co-cultures with non-parenchymal cells or dynamic cultures have also been investigated (Gebhardt et al., 2003). Under these conditions, cells exhibit a certain stability in their phenotypes. However obtaining *in vitro* metabolic activities similar to the situation found in the body remains a clear target.

In this context, progress in tissue engineering, biomaterial science and micro technologies have led to innovative cell culture conditions. Microfluidic bioreactors integrating microstructured topography and dynamic culture conditions have appeared as a potential alternative for mimicking *in vivo*-like structures (Baudoin et al., 2007; Leclerc et al., 2004). The cells cultivated in such devices can adhere to the walls of microchannels and microchambers located in bioreactors. The perfusion of culture medium inside the cell culture area improves the metabolic waste removal and continually renews the nutrient supply. Furthermore, the flow creates physiological like situations such as the liver zonation or shear stress on the hepatic tissues (Allen et al., 2005; Tilles et al., 2001). Finally, a microenvironment of a few micro litres induced by the microchambers enhances cell-cell interactions, reducing the dilution of the chemokines or other chemicals, when compared to the volume of medium involved in plate cultures (Bhatia et al., 1997; Yu et al., 2005; Bhadriraju and Chen, 2002).

In order to assess metabolic activity and/or the stability of human primary hepatocytes activity in a microfluidic biochip, the use of simultaneous administration of probes for the main enzymes responsible for drug metabolism is especially relevant. The advantages are to be able to monitor phase I (mainly CYPs) and phase II enzymes simultaneously inside the biochip. For that purpose, the CIME cocktail (Carte d'Identité MEtabolique) was designed to address the phase I enzymes CYP1A2, CYP2C8, CYP2C9, CYP2C19, CYP2D6, CYP3A, and phase II enzyme UGT 1A1 (UDP-Glucuronosyltransferase 1 polypeptide 1A). To avoid intensive biochip manipulation and parallel analysis using the substrates, a simultaneous LC–MS/MS (liquid chromatography mass spectrometry) assay of all substrates and corresponding metabolites in plasma and culture media has been developed (Videau et al., 2010). Based on this cocktail, the performances in a microfluidic environment of cryopreserved human primary hepatocytes were assessed and compared to metabolic activities in plate cultures.

2. Materials and methods

2.1. Manufacturing and preparing the liver microfluidic biochip

The manufacturing process for the liver biochip was described in detail in our previous work (Baudoin et al., 2007). Briefly, one layer of PolyDimethylSiloxane (PDMS) containing microstructured channels interconnected with a larger microchamber is bound to a second PDMS replica in order to obtain a closed biochip. The chamber volume is 40 μL and the area available for cell cultures represents 2 cm^2, including the microchannel walls. To enhance cell attachment, a coating is made by injecting rat tail collagen I (BD Bioscience) diluted at 300 μg/mL in PBS solution. The collagen was incubated for 2 h in a CO_2 incubator, at 37 °C. Before cell seeding, the liver microfluidic biochips were rinsed with culture medium.

Table 1
CIME cocktail composition (7 parent substrates and 10 analysed metabolites).

Substrates	Enzymes	Analysed metabolites
Midazolam	CYP3A4	1-OH-midazolam/4-OH-Midazolam
Dextromethorphan	CYP2D6 and CYP3A	Dextorphan/3-methoxymorphinan
Caffeine	CYP1A2	Paraxanthine
Tolbutamide	CYP2C9	4-OH-Tolbutamide
Acetaminophen	UGT	Acetaminophen-glucuronide
Amodiaquine	CYP2C8	Desethylamodiaquine
Omeprazole	CYP2C19 and CYP3A	5-OH-omeprazole/Omeprazole-sulfone

2.2. Chemicals and CIME cocktail composition

The Carte d'Identité MEtabolique (CIME) cocktail is composed of 7 parent substrates and we analysed 10 metabolites (Table 1) resulting of the biotransformation reactions of the 7 parent substrates.

The following substrates and metabolites used to prepare the standard solutions were obtained from Sigma–Aldrich (St. Quentin Fallavier, France): acetaminophen (CAS 103-90-2), acetaminophen glucuronide (CAS 120595-80-4) (ACEGLU), amodiaquin dihydrochloride dehydrate (CAS 6398-98-7), caffeine (CAS 58-08-2), paraxanthine (CAS 611-59-6) (PARA), dextromethorphan (CAS 6700-34-1), dextorphan-D-tartrate (CAS 143-98-6) (DXR), 3-methoxymorphinan hydrochloride (CAS 36397-14-5) (MEM), midazolam maleate salt (CAS 59467-94-6), 1′-OH midazolam (CAS 59468-90-5) (1OHMDZ), 4-OH midazolam (CAS 59468-85-8) (4OHMDZ), omeprazole (CAS 73590-58-6), and tolbutamide (CAS 64-77-7). 5-OH omeprazole (CAS 92340-57-3) (5OHOME) and 4-OH tolbutamide (CAS 5719-85-7) (4OHTOLB) were obtained from SPI-Bio (Montigny Le Bretonneux, France). Omeprazole sulfone (CAS 88546-55-8) (OMESU) was obtained from @rtMolecule (Poitiers, France), and desethylamodiaquine (CAS 79352-78-6) (DESE) was obtained from BD Biosciences (Woburn, MA, USA).

2.3. Human hepatocyte preparation

Cryopreserved hepatocytes from 2 human donors (BioPredict, Rennes, France) were warmed at 37 °C and pooled together in a 50 mL flask in 40 mL of warmed Leibowitz L15 medium. After a 50 × *g* centrifugation for 2 min, the cell pellet was suspended in a 27% percoll solution and centrifuged at 50 × *g* for 5 min. After removing the supernatant, viable cells were suspended in 2 mL of seeding medium. The seeding medium is a Williams E Glutamax medium supplemented with penicillin 100 UI/mL, streptomycin 100 μg/mL, bovine insulin 4 μg/mL and foetal calf serum 10% v/v. Viability was achieved by means of trypan blue exclusion and cell number was determined with a Malassez cell. After a final centrifugation at 50 × *g* for 4 min, was performed in order to adjust the cell concentration to the desired inoculated cell density.

2.4. Dynamic culture in liver microfluidic biochips

Hepatocytes suspended in the seeding medium were inoculated into the liver biochip at $1.1 \pm 0.1 \times 10^5$ cells/cm^2 (condition M) and placed without flow in a CO_2 incubator at 37 °C for the adhesion period (12 h). After adhesion, the cells were rinsed and connected to the perfusion circuit composed of a medium reservoir, a peristaltic pumps and PeekSil tubes (Fig. 1 shows the setup). The reservoir and the circuit were loaded with 1 mL of an incubation medium including the CIME cocktail at 20 μM. The incubation medium is a Williams E Glutamax medium supplemented with penicillin

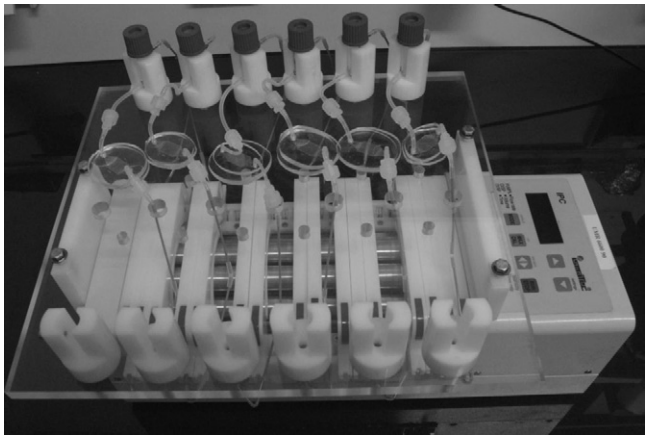

Fig. 1. Microfluidic biochip setup and peristaltic pump.

100 UI/mL, streptomycin 100 μg/mL, bovine insulin 4 μg/mL. The incubation medium containing the CIME cocktail was incubated for 1 h ($n = 3$), 3 h ($n = 3$) and 4 h ($n = 3$) in dynamic conditions. For that purpose a peristaltic pump was started at a flow rate of 20 μL/min. At the end of the incubation periods, 2 volumes of cold acetonitrile were introduced to the reservoir medium and perfusion was continued for one additional hour. All the volume (1 mL of incubation medium and 2 mL of acetonitrile) were collected. The samples including the intra and extra cellular media were stored in eppendorf tubes at −80 °C until the LC–MS/MS analysis.

2.5. Static culture in 48 well plates

Hepatocytes were seeded at 100,000 (condition P1) and 200,000 (condition P2) cells per plate in collagen I coated 48-well plates (BD Biocoat™) with a seeding medium. Cell density corresponded to $1.2 \pm 0.1 \times 10^5$ cells/cm^2 and $2.4 \pm 0.1 \times 10^5$ cells/cm^2, respectively. The cells attached overnight (12 h in the seeding medium) in a CO_2 incubator at 37 °C before exposure to the CIME cocktail.

The CIME cocktail was diluted in incubation medium at a 20 μM final concentration. 1 mL of this solution was incubated for 1 h ($n = 3$), 3 h ($n = 3$) and 4 h ($n = 3$) for each cell density. After the incubation period, 2 volumes of cold acetonitrile were added directly to 1 mL of the cocktail solution and incubated for 1 h at 37 °C. All the volume (1 mL of incubation medium and 2 mL of acetonitrile) were collected. Samples including the intra and extra cellular media were stored in eppendorf tubes at −80 °C until the LC–MS/MS analysis.

2.6. Live/dead assay

In parallel to the metabolism investigations, the cell viability was monitored at the end of the perfusion in the liver biochips ($n = 2$) and at the end of plate cultures ($n = 2$) using separate incubates. Briefly, cells were rinsed in PBS and stained with 2 μM of calcein-AM and 4 μM of propidium iodide (PI) in PBS solution for 15 min. The liver microfluidic biochip was directly observed using a conventional fluorescence microscope (Leica, LAS-AF software) with FITC and Texas red filters. Viable and dead cells appeared green and red, respectively.

2.7. CIME cocktail analysis

2.7.1. Instrumentation

The method of analysis has been presented in detail by Videau et al. (2010). Briefly, the samples were evaporated to dryness using a Turbovap LV evaporator (Zymark, Roissy, France). The dry residue was reconstituted in 400 μL of 2 mM ammonium acetate/methanol, 9/1 v/v. After vortex mixing, 20 μL was injected into the chromatographic system.

Detection and processing was performed using a Waters Acquity UPLC system that was coupled to a triple quadripole mass spectrometer Quattro Premier XE equipped with an electrospray ionization source (Waters, Saint Quentin en Yvelines, France). System control and data processing were carried out using MassLynx software, version 4.1. Quantification was performed using the QuanLynx application.

2.7.2. LC–MS/MS conditions

The peak area of all analytes was determined using a reverse phase UPLC method with tandem mass spectrometric detection according to a previously described assay (Videau et al., 2010). Samples were run on an ACQUITY UPLC® BEH Shield RP18 column (2.1 mm × 100 mm, 1.7 μM) coupled with an ACQUITY UPLC® BEH Shield RP18 1.7 μM Van Guard™ Pre-Column (Waters, St. Quentin en Yvelines, France). Mobile phases were delivered as a gradient of a first solvent composed of 0.1% formic acid in water and a second mobile phase solvent of 0.1% formic acid in acetonitrile. The flow rate was set at 0.4 mL/min. and temperatures were 50 °C and 4 °C for the column and autosampler, respectively. Run time was 8 min.

2.8. Data analysis

The metabolic ratio (MR) was defined by the ratio of the area under the curve (AUC) of the reaction products divided by the sum of all the AUC of the parent substrate and its metabolites. The equation is as follows:

$$MR_t = \frac{AUC(P)_t}{AUC(P)_t + AUC(S)_t - MR_t} \times 100$$

In which MR_t is the metabolic ratio at time t, AUC is the area under the curve of the P product of the enzymatic reaction, the S substrate and MR_0 is the initial value of metabolic ratio before the incubation.

The metabolic ratio values were calculated at each sampling time (1 h, 3 h and 4 h) for all compounds of the cocktail in order to obtain kinetic curves and illustrate the activity of the targeted enzymatic reactions. Statistical comparisons of the values of the metabolic ratio MR in biochip and plate cultures were made using a one-way ANOVA test at a P value of 0.05 and followed by Bonferroni's multiple comparison test.

3. Results

3.1. Cell morphology and viability assessment

Cell morphology after 12 h of adhesion inside the liver biochip is shown in Fig. 2A and B. 85% of the inoculated cells adhered to the biochip. The cells covered 90% of the microfluidic biochip. The cells displayed a classical polygonal shape demonstrating successful adhesion in the PDMS-coated collagen surface of the microfluidic biochip. The cell membranes appeared refractive. At the end of the 4 h perfusion period, the cell monolayer and the polygonal shapes were maintained (Fig. 2C). A live-dead assay was performed in order to assess the viability of the cells. Fig. 2D shows the double staining of viable cells (green) and necrotic cells (red) inside the microfluidic biochip. Green cells were visualized after 4 h of dynamic culture, indicating that the primary human hepatocytes were successfully cultivated in a healthy condition inside the microenvironment and in a dynamic situation.

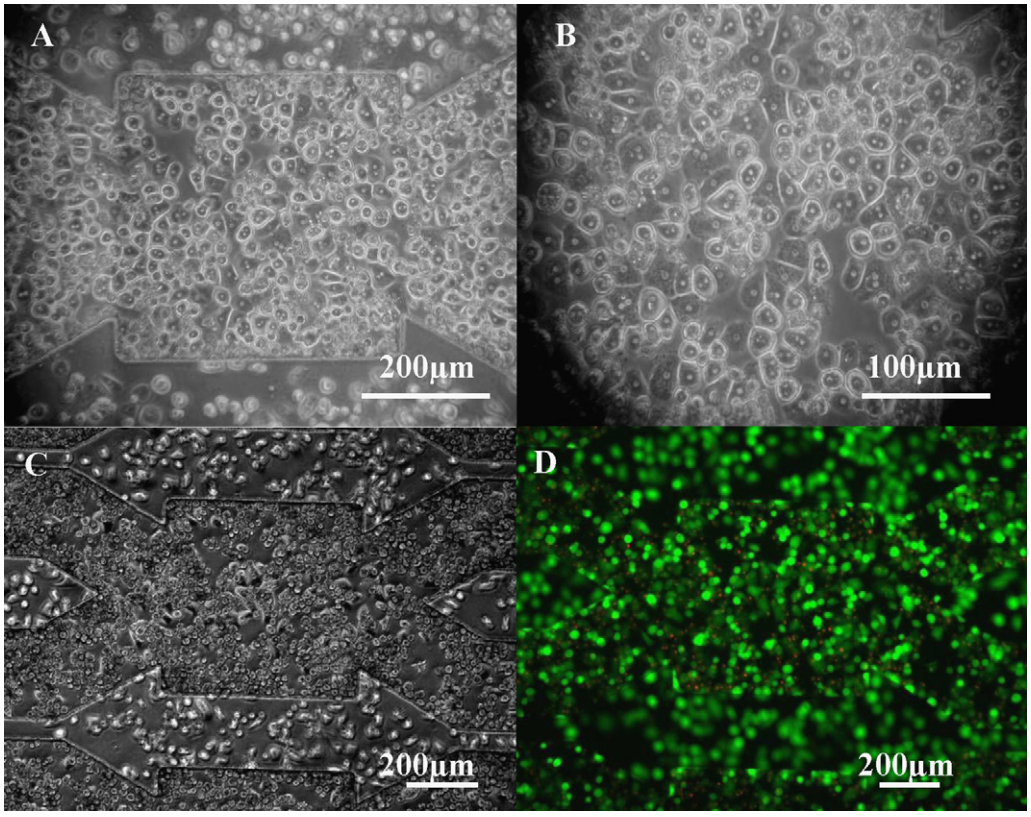

Fig. 2. (A and B) Cell morphology after 12 h of adhesion; (C) cell morphology after 16 h of culture including 12 h of adhesion and 4 h of perfusion; (D) live-dead assay after the 4 h of perfusion (green viable cells stained by Calcein AM and necrotic cells stained in red by PI). No PI positive cells were detected.

3.2. Non-specific adsorption of the cocktail compounds

Before the metabolism investigations, we studied the non-specific adsorption of the tested substrates and their metabolites diluted in the culture medium. The 17 molecules circulated in the perfusion circuit and liver biochip (without cells) for 4 h. Table 2 shows the ratio of each molecule compared to the initial concentration after 4 h of perfusion.

After 4 h of perfusion, midazolam, dextromethorphan, amodiaquine and desethylamodiaquine showed significant adsorption rates. Caffeine, acetaminophen, tolbutamide, omeprazole and their metabolites were not adsorbed over time.

Table 2
Non-specific binding of parent substrates and the metabolites after 4 h of perfusion inside the perfusion circuit. The results represent the percentage of compound remaining in the culture medium after the perfusion period reported to the initial solution ($n = 3$, mean ± SD).

Molecules	4 h
Midazolam	37.0 ± 17.7
1-OH-Midazolam	79.1 ± 8.7
4-OH-Midazolam	76.6 ± 8.8
Dextromethorphan	12.0 ± 22.4
Dextorphan	76.3 ± 7.3
3-Methoxymorphinan	59.2 ± 13.7
Caffeine	101.2 ± 7.4
Paraxanthine	103.1 ± 4.1
Tolbutamide	120.7 ± 3.4
4-OH-Tolbutamide	79.7 ± 3.4
Acetaminophen	100.4 ± 8.3
Acetaminophen-glucuronide	71.8 ± 24.4
Amodiaquine	19.3 ± 48.7
Desethylamodiaquine	6.9 ± 85.4
Omeprazole	95.1 ± 5.8
5-OH-omeprazole	99.0 ± 4.3
Omeprazole-sulfone	101.7 ± 3.6

3.3. Metabolic activity in the liver microfluidic biochip and in plate

The kinetics for the appearance of the metabolites, illustrating the targeted enzymatic reactions, are shown in Fig. 3. The production of the metabolites was measured at 1 h, 3 h and 4 h of culture in the biochip and in both static conditions for the 7 parent substrates.

Among the metabolites of the tested substrates, paraxanthine (Fig. 3C) and methoxymorphinan (Fig. 3G) production appeared to be higher in the liver biochip after the first hour of incubation. We did not distinguish any significant difference after one hour of incubation concerning the production of acetaminophen glucuronide (Fig. 3E), desethylamodiaquine (Fig. 3F), dextorphan (Fig. 3H), 5-OH omeprazole (Fig. 3I) and omeprazole–sulfone (Fig. 3J) in the microfluidic biochip when compared to the plate conditions.

Then, after one hour of incubation, stabilized production was observed for several molecules in the static "P1" condition ($1.2 \pm 0.1 \times 10^5$ cells/cm^2). The appearance of paraxanthine (Fig. 3C), methoxymorphinan (Fig. 3G), 5-OH omeprazole (Fig. 3I) and omeprazole-sulfone (Fig. 3J) reached a plateau. Thus, the production appeared constant over time for the whole duration of the experiment. This phenomenon was not observed in the liver biochip ($1.1 \pm 0.1 \times 10^5$ cells/cm^2) or in the static "P2" condition ($2.4 \pm 0.1 \times 10^5$ cells/cm^2). The metabolite production increased in the biochip between 1 h and 4 h of exposure, as illustrated by the production of paraxanthine (Fig. 3C), 4-OH-tolbutamide (Fig. 3D), acetaminophen glucuronide (Fig. 3E), desethylamodiaquine (Fig. 3F), 3-methoxymorphinan (Fig. 3G), dextrophan (Fig. 3H), and 5-OH omeprazole (Fig. 3I). As an exam-

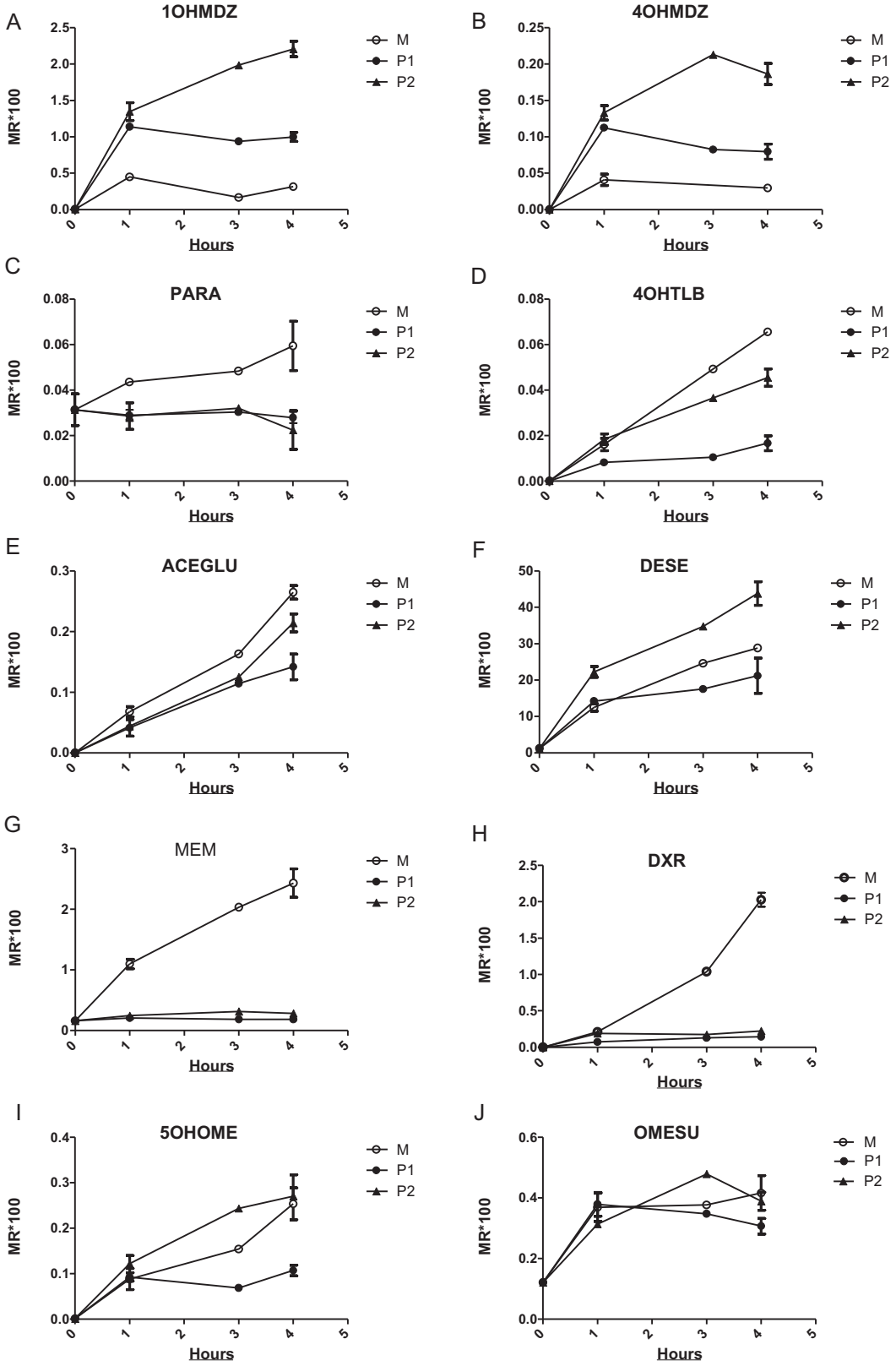

Fig. 3. Kinetics of metabolites appearance illustrating the metabolic activity in the Liver microfluidic biochip (M: $1.1 \pm 0.1 \times 10^5$ cells/cm^2) and plate cultures (P1: $1.2 \pm 0.1 \times 10^5$ cells/cm^2; P2: $2.4 \pm 0.1 \times 10^5$ cells/cm^2). (A) 1-OH-midazolam; (B) 4-OH-midazolam; (C) paraxanthine; (D) 4-OH-tolbutamide; (E) acetaminophen glucuronide; (F) desethylamodiaquine; (G) 3-methoxymorphinan; (H) dextorphan; (I) 5-OH-omeprazole; (J) omeprazole-sulfone.

ple, in the biochip, the metabolic ratio for 5-OH-omeprazole was multiplied by 2.6 between 1 h and 4 h of incubation.

After 4 h of incubation, the metabolite productions reached in liver biochips were higher than those measured in the plate P1 and P2 conditions with regard to the production of acetaminophen glucuronide (Fig. 3E), 4-OH-tolbutamide (Fig. 3D), 3-methoxymorphinan (Fig. 3G), and dextrophan (Fig. 3H). Dextrophan production was found to be higher in the biochip despite significant adsorption of the parent dextromethorphan. Productions reached in the liver biochip were at comparable levels to the plate "P2" condition with regard to the production of 5-OH omeprazole and omeprazole-sulfone (Fig. 3I and J). Finally, lower values were observed in the biochip for the production of 1-OH-midazolam and 4-OH-midazolam when compared to both plate conditions (Fig. 3A and B).

3.4. Comparison of the metabolic ratio after 4 h

Fig. 4 shows the metabolic ratio of all compounds after 4 h of incubation compared for the 3 conditions tested (biochip "M", plate "P1" and "P2"). The results were expressed in terms of metabolic ratio normalized by the initial cell number. When we compared the metabolic ratio in the plate conditions, we did not observe any significant difference between the 2 groups after 4 h of culture. We could not separate the two plate conditions, as illustrated by midazolam or omeprazole metabolism (Fig. 4A, B, I and J). Interestingly, the metabolic ratio appeared to be higher in the liver biochip when compared to the plate conditions for 5 out of 7 substrates: dextromethorphan (Fig. 4G and H), caffeine (Fig. 4C), tolbutamide (Fig. 4D), acetaminophen (Fig. 4E) and omeprazole (Fig. 4I and J). These results suggest that the enzymatic reactions related to CYP3A4, CYP2D6, CYP1A2, CYP2C9, UGTs and CYP2C19 activities were more effective in the liver biochip when compared to the plate conditions. These results were also in agreement with the significant production of the specific metabolites when compared to the plate conditions.

Midazolam and amodiaquine (Fig. 4A, B and F) were 2 substrates with high adsorption. They are metabolized by CYP3A4 and CYP2C8 respectively. However, they exhibited two different results. The production of 1-OH midazolam and 4-OH midazolam was lower in the liver biochip when compared to the plate cultures (Fig. 4A and B). On the contrary, despite the high adsorption of amodiaquine and its metabolite (desethylamodiaquine), the metabolic ratio related to CYP2C8 via desethylamodiaquine production was similar in the biochip and plate cultures (Fig. 4F).

4. Discussion

An important issue in toxicity and pharmacology studies is the development of *in vitro* tests that may provide an alternative to animal trials or able to mimic accurately what happens in Human. The current developments in tissue engineering and microtechnology fields are making it possible to propose new pertinent microtools for *in vitro* investigation to predict xenobiotic toxicity and/or metabolism. Microfluidic biochips offer the advantage of including the complete set of these technologies. They effectively offer the possibility of dynamic cultures and kinetic studies on microstructured tissues, simulating the cell organization found *in vivo* more closely than conventional plate dishes. In the present study, we have shown that human primary hepatocytes were successfully cultivated under flow conditions in the PDMS collagen-coated biochip developed in our laboratory. Our results obtained in the PDMS biochip appeared consistent with the literature reports in which primary hepatocytes were also successfully cultivated in polystyrene/polycarbonate microfluidic devices. The adhesion performance of 85% in our PDMS biochip and the resulting viability after perfusion appeared to be similar to the results in the study by (Chao et al., 2009).

Another key point, when developing new devices for cell culture in toxicology, is the absence or control of the adsorption of the molecules to be tested especially for pharmaceuticals which are often lipophilic and/or basic drugs. As the surface of the perfusion circuit and the components is larger in biochips than in classical cultures, this aspect needs to be addressed before performing the real tests. Midazolam, dextromethorphan and amodiaquine were the most adsorbed parent substrates in the perfusion system. The four other parents, caffeine, tolbutamide, acetaminophen and omeprazole, remained none-adsorbed during the perfusion period. After 4 h circulating in the perfusion circuit, the metabolites had an adsorption of less than 25%, except for desethylamodiaquine (more than 80%) and 3-methoxymorphinan (40%). The parameters promoting the molecules' adsorption are the liposolubility, polarity and non-ionization of the molecules. To pass through the cell membrane, most drugs should exhibit some apolar and lipohilic properties. In addition, ionic forms of molecules cannot pass through a biological membrane. In xenobiotic biotransformation, glutathione, glucuronosyl- and sulfotransferases enhance the molecule's polarity and solubility by adding functional hydrophilic compounds to the molecules. When considering each substrate of the cocktail, it appeared that the most adsorbed molecules were those that were apolar (*i.e.* midazolam, dextromethorphan and amodiaquine). On the contrary, polar molecules such as caffeine, acetaminophen, tolbutamide and polar metabolites were not absorbed. Omeprazole, which is a weakly polar amphoter, showed little adsorption. In the literature, the high adsorption of molecules in the perfusion circuit was also illustrated in microfluidic biochip cultures with other substrates: buspirone (buspirone hydrochloride, polar), timolol (polar), carbamazedine (polar), imipramine (imipramine hydrochloride, polar) and sildenafil, when those molecules where flowing in silicone pipes. The authors reduced adsorption by using "PeekSil" pipes for the perfusion circuit (Chao et al., 2009; Novik et al., 2010). It can be noticed that they presented the reduction in adsorption with regard to polar molecules. Our results appeared consistent. Indeed, in our study, perfusion was also done in "PeekSil" tubes in which any adsorption of the polar molecules in the CIME cocktail was also found.

To carry out *in vitro* hepatotoxicity tests or to investigate xenobiotic metabolisms, it is necessary to define animal or human cell models that express hepatic functions similar to *in vivo* conditions (Guillouzo, 1998). In this context, primary human hepatocyte co-cultures with fibroblasts on PDMS micropatterned surfaces have shown high inductions of phase I and phase II enzymes involved in metabolism (Khetani and Bhatia, 2008). Phase I and phase II enzyme inductions were also observed with rat primary hepatocytes cultivated in a Silicon microfluidic biochip (Sivaraman et al., 2005). Applied to drug metabolism studies, a liver biochip (made of polystyrene/polycarbonate) using a co-culture of human primary hepatocytes with non-parenchymal cells displayed higher metabolite production rates when compared to static co-cultures and when compared to dynamic primary hepatocyte monocultures (Chao et al., 2009; Novik et al., 2010). The improvement in the metabolic ratio in such biochips included enzymatic reactions related to CYP1A2, CYP2C8/9, CYP3A4, CYP2B6, CYP2D6, SULT and UGT activities caused by the specificity of the substrates. In addition, in hepatocyte monocultures, their results have shown higher (or similar) metabolic ratios in static cultures when compared to dynamic cultures concerning CYP1A2, CYP2C8/9, CYP3A4, CYP2B6, CYP2D6 after 24 h of culture (Chao et al., 2009; Novik et al., 2010). We performed a simpler culture protocol, in which a monoculture of hepatocytes (instead of a co-culture) was cultivated in the PDMS biochip. In our configuration, we found similar types of per-

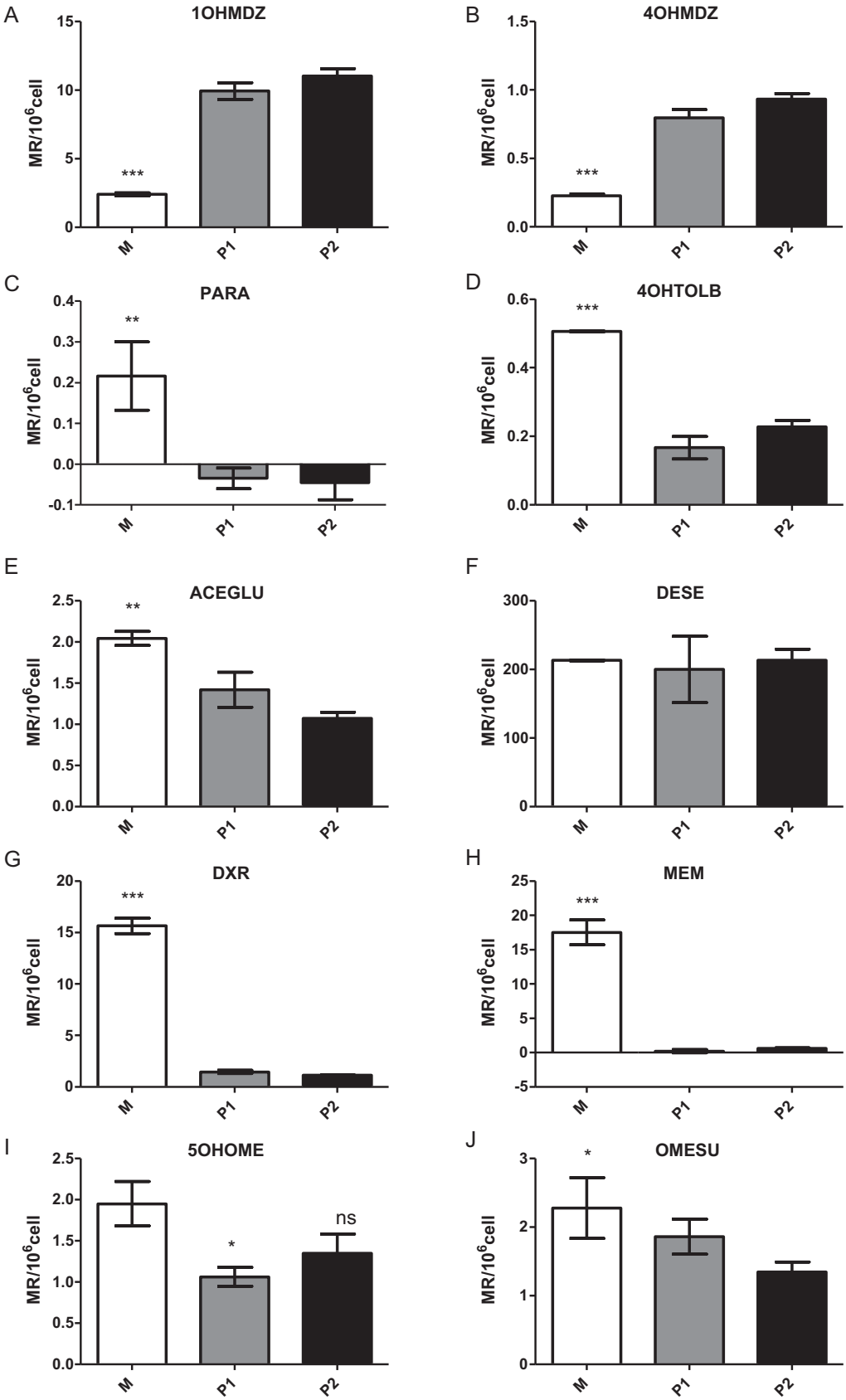

Fig. 4. Metabolic ratio comparison between liver microfluidic biochip (M: $1.1 \pm 0.1 \times 10^5$ cells/cm^2) and plate cultures (P1: $1.2 \pm 0.1 \times 10^5$ cells/cm^2; P2: $2.4 \pm 0.1 \times 10^5$ cells/cm^2). (A) 1-OH-midazolam; (B) 4-OH-midazolam; (C) Paraxanthine; (D) 4-OH-tolbutamide; (E) acetaminophen glucuronide; (F) desethylamodiaquine; (G) 3-methoxymorphinan; (H) dextorphan; (I) 5-OH-omeprazole; (J) omeprazole-sulfone.

formance as in their co-culture configuration over the 4 h of culture. Indeed, we reached a higher activity in our PDMS microfluidic biochip concerning CYP1A2, CYP2C8/9, CYP3A, CYP2D6, and UGT activities when compared to plate cultures.

In addition, even if the metabolism of the midazolam was found to be weaker in the biochip than in plate conditions, omeprazole sulfone and 3-methoxymorphinan metabolic rates demonstrated high CYP3A activity in the biochip. This difference between the CYP3A substrates can be explained by the rapid production of 1-OH midazolam and 4-OH midazolam and the following glucurono conjugation (Vossen et al., 2007; Hylan et al., 2009). Indeed, the over activation of the glucuronidation pathway has been demonstrated thanks to the acetaminophen glucurono conjugate appearance that was found higher in biochip when compared to plates. Similar process occurred after CYP3A biotransformation of dextromethorphan into 3-Methoxymorphinan that is lately metabolized by CYP2D6 and by UGT to 3-hydroxymorphinan and to 3-hydroxymorphinan-O-glucuronide (Kerry et al., 1994; Strauch et al., 2009). However when compared to midazolam, this process is slower in the dextromethorphan metabolism and is characterized by a lower Km values involved in the midazolam metabolism (namely Km = 2 μM and 0.2 μM for the 1-OH midazolam and the 1-OH midazolam-Glu formations, Vossen et al., 2007, whereas Km = 633–977 μM concerning the dextromethorphan N-demethylation to 3-methoxymorphinan). Concerning the omeprazole, the omeprozole sulfone can be lately metabolized in 5 hydroxyomeprazole-sulfone (CYP 2C19) and in pyridine-N-oxide omeprazole sulfone (CYP 3A4) at high values (ranging from 7.6 to 426 μM and 40 to 620 μM respectively according to the molecule affinity, Abelo et al., 2000; Andersson et al., 1994). Thus, based on the Km analysis we can explain partially the resulting higher CYP3A activity in omeprazole and dextromethorphan metabolism when compared to midazolam biotransformation.

The global enzyme activities in the biochip appeared consistent with our previous investigations with HepG2/C3a in a PDMS microfluidic biochip in which the phase I (CYP1A1, 2B6, 3A4, 3A5, 3A7), phase II (SULT1A1, SULT1A2, UGT1A1, UGT2B7) and phase III (MDR1, MRP2) enzymes involved in xenobiotic metabolism were found to be up regulated when compared to plate static cultures (Prot et al., 2011). This thus highlights the fact that primary hepatocyte culture in our microfluidic biochip configuration made it possible to enhance the metabolic activity of the hepatocytes by maintaining hepatic differentiation without using complex co-culture systems or spheroid formation. Finally, the potential of high enzyme induction in microfluidic biochips is illustrated by the functionality of the biotransformation process measured with the CIME cocktail. The CIME cocktail made it possible to monitor phase I and phase II enzymes simultaneously inside the biochip in one set of experiments. Besides the proof of concept for the biochip, this operation could thus be used as a routine assay for evaluating microfluidic culture performance before running drug screening analyses. Furthermore, *in vitro* exposure to the CIME cocktail can reproduce the *in vivo* situation resulting in treatments in which several drug substrates from several of these enzymes are often given to a patient simultaneously.

5. Conclusion

In summary, we successfully performed primary human hepatocyte culture inside a liver microfluidic biochip. The biochip made healthy dynamic culture conditions possible. We investigated the production rate of 10 metabolites, resulting in the conversion of a cocktail of 7 parent substrates. The cocktail made rapid hepatocyte profiling possible, as well as metabolic characterisation, using a single detection technique. Seven of the 10 metabolites tested in this study showed a higher production rate in the liver microfluidic biochip than in conventional culture methods. Despite adsorption, we showed that dynamic culture conditions and the microenvironment of the liver microfluidic biochip resulted in higher activity of the enzymes involved in xenobiotic metabolism. This led to higher xenobiotic conversion for 5 of the 7 substrates tested. Thus, the microfluidic biochip appeared to be a sensitive new culture method using primary human hepatocytes for future models for pharmaceutical drug screening and toxicity analysis of xenobiotics.

Acknowledgements

Jean Matthieu Prot received a grant from the CNRS and "Région Picardie". The project was supported by the Foundation of the University of Technology of Compiègne "La Fondation UTC pour l'innovation". We thank Laurent Griscom from Biomis/Satie CNRS UMR 8089 who fabricated the mould master of the microfluidic biochip. We thank Eric Ezan from CEA Saclay, Laboratoire d'Etude du Métabolisme et du Médicament, for his helpful advices during the redaction.

References

Abelo, A., Anderson, T., Antonsson, M., Knuts Naudot, A., Skanberg, I., Weidolf, L., 2000. Stereoselective metabolism of omeprazole by Human cytochrome P450 enzymes. Drug Metab. Dispos. 28, 966–972.

Andersson, T., Miners, J., Veronese, M., Birkett, D., 1994. Identification of human liver cytochrome P450 isoforms mediating secondary omeprazole metabolism. Br. J. Clin. Pharmac. 37, 597–604.

Allen, J.W., Khetani, S.R., Bhatia, S.N., 2005. Zonation and toxicity in a hepatocyte bioreactor. Toxicol. Sci. 84, 110–119.

Baillie, T.A., 2006. Future of toxicology-metabolic activation and drug design: challenges and opportunities in chemical toxicology. Chem. Res. Toxicol. 19, 889–893.

Baudoin, R., Griscom, L., Monge, M., Legallais, C., Leclerc, E., 2007. Development of a renal microchip for *in vitro* distal tubule models. Biotechnol. Prog. 23, 1245–1253.

Bhadriraju, K., Chen, C.S., 2002. Engineering cellular microenvironments to improve cell-based drug testing. Drug Discov. Today 7, 612–620.

Bhatia, S.N., Yarmush, M.L., Toner, M., 1997. Controlling cell interactions by micropatterning in co-cultures: hepatocytes and 3T3 fibroblasts. J. Biomed. Mater. Res. 34, 189–199.

Brandon, E.F.A., Raap, C.D., Meijerman, I., Beijnen, J.H., Schellens, J.H.M., 2003. An update on *in vitro* test methods in human hepatic drug biotransformation research: pros and cons. Toxicol. Appl. Pharmacol. 189, 233–246.

Chao, P., Maguire, T., Novik, E., Cheng, K.C., Yarmush, M.L., 2009. Evaluation of a microfluidic based cell culture platform with primary human hepatocytes for the prediction of hepatic clearance in human. Biochem. Pharmacol. 78, 625–632.

Erve, J.C.L., 2006. Chemical toxicology: reactive intermediates and their role in pharmacology and toxicology. Expert Opin. Drug Metabol. Toxicol. 2, 923–946.

Gebhardt, R., Hengstler, J.G., Muller, D., Glockner, R., Buenning, P., Laube, B., Schmelzer, E., Ullrich, M., Utesch, D., Hewitt, N., Ringel, M., Hilz, B.R., Bader, A., Langsch, A., Koose, T., Burger, H.J., Maas, J., Oesch, F., 2003. New hepatocyte *in vitro* systems for drug metabolism: metabolic capacity and recommendations for application in basic research and drug development, standard operation procedures. Drug Metab. Rev. 35, 145–213.

Gomez-Lechon, M.J., Castell, J.V., Donato, M.T., 2007. Hepatocytes-the choice to investigate drug metabolism and toxicity in man: *in vitro* variability as a reflection of *in vivo*. Chem. Biol. Interact. 168, 30–50.

Guillouzo, A., 1998. Liver cell models in *in vitro* toxicology. Environ. Health Perspect. 106, 511–532.

Guillouzo, A., Morel, F., Langouët, S., Maheo, K., Rissel, M., 1997. Use of hepatocyte cultures for the study of hepatotoxic compounds. J. Hepatol. 26, 73–80.

Hewitt, N.J., Hewitt, P., 2004. Phase I and II enzyme characterization of two sources of HepG2 cell lines. Xenobiotica 34, 243–256.

Hewitt, N.J., Lechón, M.J.G., Houston, J.B., Hallifax, D., Brown, H.S., Maurel, P., Kenna, J.G., Gustavsson, L., Lohmann, C., Skonberg, C., Guillouzo, A., Tuschl, G., Li, A.P., LeCluyse, E., Groothuis, G.M.M., Hengstler, J.G., 2007. Primary hepatocytes: current understanding of the regulation of metabolic enzymes and transporter proteins, and pharmaceutical practice for the use of hepatocytes in metabolism, enzyme induction, transporter clearance, and hepatotoxicity studies. Drug Metab. Rev. 39, 159–234.

Hylan, R., Osborne, T., Payne, A., Kemshall, S., Logan, R., Ezzeddine, K., Jones, B., 2009. *In vitro* and *in vivo* glucuronidation of midazolam in humans. Br. J. Clin. Pharmacol. 67, 445–454.

Kedderis, G.L., Held, S.D., 1996. Prediction of furan pharmacokinetics from hepatocyte studies: comparison of bioactivation and hepatic dosimetry in rats, mice, and humans. Toxicol. Appl. Pharmacol. 140, 124–130.

Kerry, N.L., Somogyi, A., Bochner, F., Mikus, G., 1994. The role of CYP2D6 in primary and secondary oxidative metabolism of dextromethorphan: *in vitro* studies using human liver microsomes. Br. J. Clin. Pharmacol. 38, 243–248.

Khetani, S.R., Bhatia, S.N., 2008. Microscale culture of human liver cells for drug development. Nat. Biotechnol. 26, 120–126.

Kienhuis, A.S., Wortelboer, H.M., Maas, W.J., van Herwijnen, M., Kleinjans, J.C.S., van Delft, J.H.M., Stierum, R.H., 2007. A sandwich-cultured rat hepatocyte system with increased metabolic competence evaluated by gene expression profiling. Toxicol. Vitro. 21, 892–990.

Lau, Y.Y., Sapidou, E., Cui, X., White, R.E., Cheng, K.C., 2002. Development of a novel in vitro model to predict hepatic clearance using fresh cryopreserved and sandwich-cultured hepatocytes. Drug Metab. Dispos. 30, 1446–1454.

Leclerc, E., Sakai, Y., Fujii, T., 2004. Microfluidic PDMS (polydimethylsiloxane) bioreactor for large-scale culture of hepatocytes. Biotechnol. Prog. 20, 750–755.

LeCluyse, E.L., 2001. Human hepatocyte culture systems for the *in vitro* evaluation of cytochrome P450 expression and regulation. Eur. J. Pharm. Sci. 13, 343–368.

Lipscomb, J.C., Poet, T.S., 2008. *In vitro* measurements of metabolism for application in pharmacokinetic modeling. Pharmacol. Ther. 118, 82–103.

Maurel, P., 1996. The use of adult human hepatocytes in primary culture and other *in vitro* systems to investigate drug metabolism in man. Adv. Drug Deliv. Rev. 22, 105–132.

Novik, E., Maguire, T.J., Chao, P., Cheng, K.C., Yarmush, M.L., 2010. A microfluidic hepatic coculture platform for cell-based drug metabolism studies. Biochem. Pharmacol. 79, 1036–1044.

Prot, J.-M., Aninat, C., Griscom, L., Razan, F., Brochot, C., Guguen Guillouzo, C., Legallais, C., Corlu, A., Leclerc, E., 2011. Improvement of HepG2/C3a cell functions in a microfluidic biochip, Biotechnol. Bioeng., in press.

Richert, L., Abadie, C., Bonet, A., Heyd, B., Mantion, G., Alexandre, E., Bachellier, P., Kingston, S., Pattenden, C., Illouz, S., Dennison, A., Hoffmann, S., Coecke, S., 2010. Inter-laboratory evaluation of the response of primary human hepatocyte cultures to model CYP inducers – A European Centre for Validation of Alternative Methods (ECVAM) – funded pre-validation study. Toxicol. Vitro. 24, 335–345.

Sivaraman, A., Leach, J.K., Townsend, S., Iida, T., Hogan, B.J., Stolz, D.B., Fry, R., Samson, L.D., Tannenbaum, S.R., Griffith, L.G., 2005. A microscale *in vitro* physiological model of the liver: predictive screens for drug metabolism and enzyme induction. Curr. Drug. Metab. 6, 569–591.

Soars, M.G., McGinnity, D.F., Grime, K., Riley, R.J., 2007. The pivotal role of hepatocytes in drug discovery. Chem. Biol. Interact. 168, 2–15.

Strauch, K., Lutz, U., Bittner, N., Lutz, W., 2009. Dose–response relationship for the pharmacokinetic interaction of grapefruit juice with dextromethorphan investigated by human urinary metabolite profiles. Food Chem. Toxicol. 47, 1928–1935.

Tilles, A., Baskaran, H., Roy, P., Yarmush, M., Toner, M., 2001. Effects of oxygenation and flow on the viability and function of rat hepatocytes cocultured in a microchannel flat-plate bioreactor. Biotech. Bioeng. 73, 379–389.

Videau, O., Delaforge, M., Levi, M., Thévenot, E., Gal, O., Becquemont, L., Beaune, P., Bénech, H., 2010. Biochemical and analytical development of the CIME cocktail for drug fate assessment in humans. Rapid Commun. Mass Spectrom. 24, 2407–2419.

Vossen, M., Sevestre, M., Niederalt, C., Jang, I., Willmann, S., Edginton, A.N., 2007. Dynamically simulating the interaction of midazolam and the CYP3A4 inhibitor itraconazole using individual coupled whole-body physiologically based pharmacokinetic (WB-PBPK) models. Theor. Biol. Med. Modell. 4, 1–15.

Yu, H., Meyvantsson, I., Shkel, I.A., Beebe, D.J., 2005. Diffusion dependent cell behavior in microenvironments. Lab Chip. 5, 1089–1095.